Comparison of structures and cytotoxicity of mupirocin and batumin against melanoma and several other cancer cell lines

SCHOLARONE™
Manuscripts

Comparison of structures and cytotoxicity of mupirocin and batumin against melanoma and several other cancer cell lines

Oleg N Reva[*,1], Sunelle Rademan[2], Michelle H Visagie[3], Maphuti T Lebelo[3], Mokgadi V Gwangwa[3], Vitalii V Klochko[4], Anna M Joubert[3] & Namrita Lall[2]

[1]Department of Biochemistry, Genetics & Microbiology, Centre for Bioinformatics & Computational Biology, University of Pretoria, Pretoria 0002, South Africa
[2]Department of Plant & Soil Sciences, Medicinal Plant Science Section, University of Pretoria, Pretoria 0002, South Africa
[3]Department of Physiology, University of Pretoria, Pretoria 0001, South Africa
[4]Department of Antibiotics, D.K. Zabolotny Institute of Microbiology & Virology, National Academy of Science of Ukraine, Kyiv 03680, Ukraine

*Author for correspondence: oleg.reva@up.ac.za

Abstract

Aim: To determine the computer-predicted anticancer activity of mupirocin and to compare its activities with those determined for another polyene antibiotic, batumin. **Materials & methods:** Molecular docking, cytotoxicity assays, cell microscopy and cell cycle progression were studied in cancer and non-tumorigenic cell lines. **Results & conclusions:** Cytotoxicity of mupirocin against several cancerous cell lines was detected with the highest one ($IC_{50} = 5.4$ μg/ml) against melanoma cell line. The profile of cytotoxicity of mupirocin was similar to that reported for batumin. Nevertheless, the morphology of cells treated with these antibiotics and alterations in cell cycle progression suggested possible dissimilarity in their mechanisms of action. Selective cytotoxicity of mupirocin against melanoma cells potentiates further studies to discover non-toxic drugs for melanoma prevention.
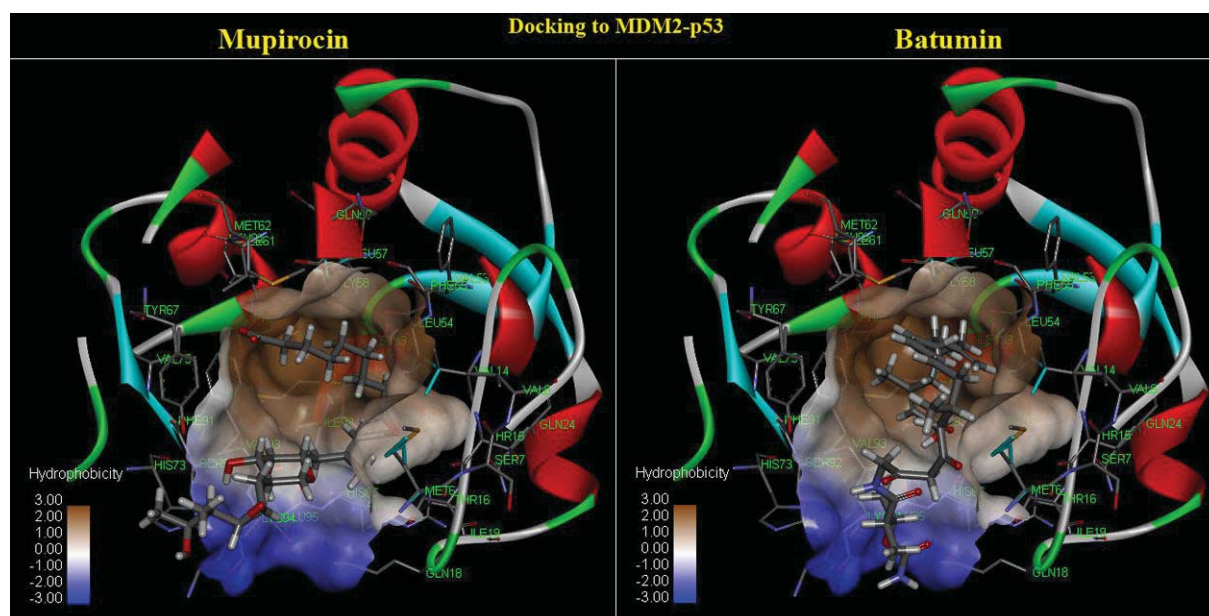
Keywords: mupirocin; batumin; melanoma; molecular docking; drug design; prophylaxis

Introduction

Malignant melanoma is a major cause of death from skin cancer worldwide. Melanoma skin cancer has a high tendency to spread to other parts of the body where it becomes difficult to treat and it can be fatal. It is reported by the World Health Organization that 132,000 cases of skin cancer occur on an annual basis. In 2016, an estimate of 76,380 skin cancer cases will be invasive melanomas with about 46,870 in males and 29,510 in women (Skin Cancer Foundation – https://www.skincancer.org/, 2018). It is further envisaged that there will be an annual increase of skin cancer incidences by 4,500 as result of the 10% destruction of the ozone layer.

Malignant melanoma is provoked by ultraviolet exposure and sunburns especially if individuals are genetically predisposed to this disease. Five or more sunburns double the risk of melanoma development [1]. South Africa and Australia have the highest rate of malignant melanoma in the world due to the elevated UV radiation index in the southern hemisphere [2]. Currently, no drugs are available for melanoma prevention after sunburns. The only recommendation is to inspect the skin regularly for early detection of possible malformations [3, 4]. High toxicity of anticancer chemotherapy hampers using these medicines for cancer prophylaxis. Probably only one exception is the reported successful application of tamoxifen for breast cancer prevention [5]. Discovery of new bioactive compounds expressing highly selective anticancer activity is of great demand for cancer treatment and prophylaxis.

Recently we have discovered a promising culture-specific anticancer activity of a polyene antibiotic, batumin, synthesized by *Pseudomonas batumici* [6], which initially had been introduced as an antibiotic against *Staphylococcus aureus* [7-9]. Although there are many distinctions in the chemical structures of batumin and mupirocin (molecular formula of mupirocin is $C_{26}H_{43}O_9$ and that of batumin is $C_{30}H_{48}N_2O_7$); recently published results of molecular docking suggested that mupirocin, also known as pseudomonic acid A, might have similar molecular targets [10]. Mupirocin suppresses growth of *S. aureus* by binding to the Rossmann fold domain of IleRS that leads to an inhibition of protein synthesis in susceptible bacteria [11, 12]. Strong affinity of batumin to IleRS was predicted by computer simulations [10]. However, the hypothesis of identity of molecular targets of mupirocin and batumin was criticized in another publication because of obviously distinct effects of these antibiotics on

protein and fatty acid biosynthesis in *S. aureus* [13]. By contrast to mupirocin, batumin inhibits predominantly the synthesis of fatty acids despite the predicted strong affinity to isoleucyl- and leucyl-tRNA synthetases involved in protein synthesis.

Possible anticancer activities of mupirocin and batumin were predicted by computer-based molecular docking. Later on, a promising culture-specific cytotoxicity against melanoma and several other cancerous cell lines and an anti-metastatic activity were demonstrated experimentally for batumin [6]. Providing that mupirocin has a similar anti-melanoma activity, this drug can be even of a higher practical importance in terms of melanoma prophylaxis due to the long history of successful application of mupirocin in the topical ointment Bactroban™ [14-19].

Considering the importance of discovery of new effective and non-toxic drugs for melanoma prophylaxis, it was decided to conduct an experimental trial to evaluate the possible anticancer activity of mupirocin using the research protocol which was previously applied to study the anticancer activities of batumin [6]. This study includes molecular docking of mupirocin against active centers of cancer related proteins p53 and Act1; performing cytotoxicity assays on several cancerous cell lines, light microscopy cell morphology and cell cycle progression analysis by means of flow cytometry. All discovered activities of mupirocin were compared to those obtained for batumin.

Both mupirocin and batumin are linear polyene antibiotic encoded by large hybrid operons of polyketide synthases and nonribosomal peptide synthetase (PKS-NRPS) comprising multiple genes [9, 21]. Natural PKS-NRPS encoded polyenes are versatile in their chemical structures and biological activities [22], which include many potential and clinically approved antibacterial, antiviral, antifungal and anti-cancer drugs [23]. Polyene antibiotics are convenient products for further genetic engineering as all their structural versatility can be designed by manipulations with a limited number of functional building units [24]. Hence, knowledge of molecular mechanisms of action of bioactive polyene compounds will aid in design and optimization of new drugs for cancer treatment and prophylaxis.

Materials & methods

Mupirocin and batumin

Mupirocin was obtained from Sigma-Aldrich (St. Louis, MO, USA; M7694-50MG). Batumin was provided by D.K. Zabolotny Institute of Microbiology and Virology, Kyiv, Ukraine. Batumin was synthesized and purified as described previously [6, 25].

In silico molecular docking

The chemical structures of mupirocin and batumin have been described in previous publications [7, 9, 10, 21]. Accelrys Discovery Studio 4.0 was used to generate a collection of spatial conformations of mupirocin and batumin, which were then used for querying the PharmaDB database containing more than 140,000 pharmacophore models [26]. Thereafter, the molecular docking of molecules of mupirocin and batumin was performed against identified target proteins by using the LibDock algorithm [27]. Chemical structures of the target proteins in PDB format with identified binding sites and chemical structures of known inhibitors were obtained from the Research Collaboratory for Structural Bioinformatics Protein Data Bank (RCSB PDB) database (www.rcsb.org, [28]) under the accession numbers 2X0U, 2X0V and 4QO4 for the Mouse Double Minute 2 (MDM2) active center of the protein p53; 3CQW and 4GV1 for the Akt1 protein.

Cancerous cell lines

The human epidermoid carcinoma (A431); human cervical adenocarcinoma (HeLa) and human epithelial metastatic (pleural effusion) mammary gland breast adenocarcinoma (MCF-7) cell lines were obtained from the European Collection of Cell Cultures (ECACC, England, UK). The human pigmented melanocyte metastatic (inguinal lymph node) melanoma (UCT-Mel 1) and human spontaneously transformed immortalized skin keratinocyte (HaCat) cell lines were generously donated by Prof. Lester Davids from the Department of Human Biology at the University of Cape Town, RSA. Fetal bovine serum (FBS) and antibiotics were purchased from Separations (Pty) Ltd. (Randburg, Johannesburg, RSA). The Cell Proliferation Kit II (XTT),

Bouin's solution, Hematoxylin solution Gill NO. 1, Eosin Y solution (alcoholic), xylenes and all other chemicals and reagents were acquired from Sigma-Aldrich (St. Louis, MO, USA).

The MCF-7 and HeLa cell lines were maintained in Eagle's Essential Medium (EMEM). The A431, UCT-Mel 1 and HaCat cell lines were cultured in Dulbecco's Modified Eagle's Medium (DMEM). Antibiotics (100 µg/ml penicillin, 100 µg/ml streptomycin and 250 µg/l fungizone) at 1% and heat-inactivated fetal bovine serum at 10% (FBS) were used as supplements to prepare the complete growth media for all of the cell lines. The cells were grown at standard culture conditions (37°C and 5% CO_2) in a humidified incubator. Cells were sub-cultured with 0.25% (w/v) trypsin 0.53 mM ethylenediaminetetraacetic acid (EDTA) for a maximum of 15 min every 2-3 days after they had formed an 80% confluent monolayer.

In vitro cytotoxicity assay

To analyze the effect of mupirocin and batumin on cell viability, the 3-[4,5-dimethylthiazole-2-yl]-2,5-diphenyltetrazolium bromide (XTT) assay [29] was performed. Cells were seeded in 100 µl EMEM or DMEM medium depending on the cell line and in 96-well microtitre plates at a concentration of 1×10^5 cells/ml. Plates were then incubated for 24 h at 37°C and 5% CO_2 to allow cells to attach to the bottom of the wells. Stock solutions of 10 mg/ml of antibiotics were prepared. Serial dilutions were made to achieve target concentrations of antibiotics in a wide range (3.125 – 400 µg/ml) assuming that the cytotoxic activity may be culture-specific. Mupirocin was also evaluated at a concentration range of 6.25 – 800 µg/ml to obtain the IC_{50} value on the HaCat cell line. Plates were incubated with antibiotics for a further 72 h at 37°C. The control wells included vehicle-treated cells exposed to 1% dimethyl sulfoxide (DMSO); cells propagated in growth medium and cells exposed to actinomycin D [30] in a range of concentrations (0.002 – 0.5 µg/ml). Since actinomycin D was one of the first antibiotics that was discovered to have antiproliferative-, apoptotic- and anticancer activity and it's mechanism of action ultimately also exerts an effect on p53, it was considered as an appropriate positive control in this study. Subsequently, XTT reagent was added to a final concentration of 0.3 mg/ml and the plates were incubated for 2 h. A BIO-TEK Power-Wave XS multi-well plate reader (A.D.P., Weltevreden Park, South Africa) was used to read the absorbance of the color complex (wavelength = 490 nm; reference wavelength = 690 nm).

Cell morphology

UCT-Mel 1 melanoma cells were plated on heat-sterilized coverslips at a cell density of 2×10^5 cells per coverslip in 6-well plates. Following 24 h of incubation at standard culture conditions to allow for cell adherence, cells were exposed to a range of concentrations of antibiotics (4, 8 and 12 µg/ml). Cells propagated in 1% DMSO in complete DMEM growth medium and cells treated with 0.0008 µg/ml actinomycin D were included as cell toxicity negative and positive controls, respectively. Subsequently, cells were incubated at 37°C for a period of 72 h. Following the incubation period, media was discarded and cells were washed with phosphate-buffered saline (PBS). The cells were stained with the standard haematoxylin and eosin staining procedure as previously described [31]. Different types of cell death morphology were identified [32]. Microscopy slides were prepared and cells were observed under a light microscope (ZEISS, Primovert) at 20× and 40× magnification.

Cell cycle progression

Flow cytometry and propidium iodide were utilized to investigate the DNA content in order to determine the influence of the antibiotics on cell cycle progression and possible apoptosis induction. Propidium iodide stains the DNA and thus enables the quantification of DNA correlating with stages of the cell cycle during cell division [33]. HaCat and UCT-Mel 1 cells were plated at 500,000 cells per 25 cm^2 flask in DMEM containing 100 U/ml penicillin G, 100 µg/ml streptomycin with fungizone (250 µg/l) and 10% FBS (heat-inactivated for 30 min at 56ºC). After 24 h, cells were treated for 72 h at 37°C with DMEM containing 100 U/ml penicillin G, 100 µg/ml streptomycin and fungizone (250 µg/l) and 10% FBS (heat-inactivated for 30 min at 56ºC) containing the estimated half maximal inhibitory concentration (IC$_{50}$) of the evaluated antibiotics, which were either 5.4 µg/ml mupirocin or 4.5 µg/ml batumin. Vehicle-treated cells (1% DMSO) were included as a negative control and cells treated with 0.0015 µg/ml actinomycin D were included as a positive control of cell death induction. After exposure to the antibiotics, cells were trypsinized in 0.25% (w/v) trypsin with 0.53 mM EDTA for approximately 15 min or until cells were rounded and ready to detach from the flask surface. Subsequently, cells were collected in a 15 ml tube, centrifuged and resuspended in ice-cold PBS twice. Cells were resuspended in ice-cold PBS (200 µl) containing 0.1% FBS. In order to avoid

cell clumping, 4ml of ice-cold 70% ethanol was slowly added in a drop wise manner while constantly vortexing. Cells were centrifuged (5 min) and the supernatant was removed and thereafter the cells were resuspended in a PBS solution containing 40 µg/ml propidium iodide, 0.1% triton X-100 and 100 µg/ml RNase A. Samples were incubated at 37ºC in 5% CO_2 for 45 min. Subsequently sample analyses were accomplished by means of a FC500 flow cytometer Beckman Coulter (Brea, CA, USA). DNA content in each cell cycle phase was calculated by Cyflogic version 1.2.1 (Perttu Terho, Turko, Finland), which assigns relative DNA content per cell to sub-G_1, G_1, S and G_2/M phases. Flow cytometry analysis involved at least 10,000 events and was repeated three times, where the mean and the standard deviation were calculated. *P*-values less than 0.05 were regarded as statistically significant.

Statistical analysis

Statistical analysis was performed by the descriptive statistics, Student's *t*-test and Mann-Whitney U test with the use of Microsoft Excel and Microcal Origin programs. All assays were performed a minimum of three times. The fifty percent inhibitory concentrations (IC_{50}) of the compounds were calculated using the GraphPad Prism 4 program (GraphPad Software, Inc., CA, USA). The safety margins of the compounds were also taken into account by calculating the selectivity index (SI) values as a ratio of IC_{50} determined on non-cancerous cells to IC_{50} cancerous cell line. The SI value gives an indication of the specificity towards either the cancerous cell line or the non-cancerous cell line [34]. A SI value greater than one indicates a specificity towards the cancerous cell line; whereas a SI value less than one implies that the compound is more toxic towards the non-cancerous cell line.

Results

Search through PharmaDB and molecular docking

Both, mupirocin and batumin have been previously identified as anti-staphylococcal antibiotics and the chemical structures of these antibiotics were identified [8, 16-20]. The search through PharmaDB revealed possible affinities of these antibiotics to active centers of cancer related

proteins p53 and Act1 (Fig. 1). An affinity to the MDM2 active center of p53 was predicted by this method for both antibiotics. Also, mupirocin was predicted to bind to the active center of the protein Act1.

An estimation of binding energy of the compounds to the active centers of the target molecules was performed by using LibDock algorithm [27]. Instead of the structure models 2X0U, 2X0V and 3CQW from PharmaDB database, RCSB PDB models 4QO4 for MDM2-p53 [35] and 4GV1 for Act1 [36] were used. The reason for this replacement was that the latter models were provided with locations of several known inhibitors of these enzymes to be used as references during the molecular docking.

Both antibiotics showed strong affinity to these cancer-related proteins (Table 1). The binding energy was comparable with the values reported for known p53 and Act1 inhibitors [35-37]. Mupirocin showed a higher affinity to the protein Act1 that was in agreement with the PharmaDB docking prediction (Fig. 1). Blocking the MDM2-p53 active center by ligands potentially may restore apoptosis in cancer cells [38]. Inhibiting of the Act1 protein kinase disrupts the (PI3K)-Akt signaling pathway, which plays a key role in cell growth and proliferation, and usually is hyper-activated in cancerous cells [36]. A detailed analysis of non-covalent bonding between ligands and amino acid residues in the active centers of the target proteins is shown in Fig. 2. In these computational models, batumin was bound to amino acids in active centers of targeted proteins by creating hydrogen and hydrophobic bonds. In the case with mupirocin, there were more hydrogen bonds due to a higher level of oxidation of the molecule. The molecule of mupirocin contains 9 oxygen atoms (29% of the molecular weight) and 43 hydrogen atoms. In batumin, there are 7 oxygen atoms (21% of the molecular weight) and 48 hydrogen atoms. Also, both mupirocin and batumin can create strong electrostatic bonds with positively charged amino acids by means of the carboxyl groups at the 9-hydroxynonanoic acid termini of these molecules. Results of molecular docking and the corresponding conformations of mupirocin and batumin molecules are visualized in Fig. 3. Affinity of mupirocin to the enzymatic centers of cancer related proteins indicates a possible anticancer activity similar to that reported for batumin [6].

Cytotoxicity assays

Assays for the anticancer activity of antibiotics were performed by XTT approach [29]. Table 2 shows estimated IC_{50} values calculated for different cancerous cell lines used in this experiment in comparison to batumin and actinomycin D used as positive controls. Mupirocin showed the highest cytotoxic activity against the UCT-Mel 1 melanoma cell line (IC_{50} = 5.4 µg/ml) with very low toxicity against the normal skin keratinocytes HaCat (IC_{50} = 415.5 µg/ml). The profile of cytotoxic activities of mupirocin was similar to that obtained for batumin [6] except for mupirocin being 4-fold more active against the breast cancer cell line MCF-7 with IC_{50} 35.5 µg/ml compared 140.6 µg/ml estimated for batumin. Contrary, batumin was more active against the UCT-Mel 1 cells with IC_{50} = 4.5 µg/ml with relatively low cytotoxicity in relation to skin keratinocytes (IC_{50} = 101.4 µg/ml). The selectivity indices (SI) in relation to melanoma cells compared to keratinocytes were 22 for batumin, 77 for mupirocin and only 4.3 for actinomycin D.

Cell cycle progression

The effect of mupirocin on cell cycle progression was investigated by means of flow cytometry on the melanoma cell line UCT-Mel 1 and skin keratinocytes HaCat cells and compared to vehicle-treated cells (negative control) and the effects of batumin and actinomycin D. Resulted DNA content frequency diagrams are shown in Fig. 4. Thereafter, flow cytometer outputs were processed by Cyflogic 1.2.1 software package to estimate percentages of cells occupying different growth phases as shown in Table 3.

Cell cycle progression studies showed that mupirocin induced a significant increase in the quantity of cells occupying the sub-G_1 phase in both cell lines UCT-Mel 1 and HaCat indicating the induction of cell death. The histogram depicting DNA content after the treatment with mupirocin resembles that of the treatment with actinomycin D but differed from the effect of batumin (Table 3 and Fig. 4). Exposure to batumin at the same conditions showed a more prominent effect on the cell cycle progression of melanoma cells than when compared to the HaCat cell line. Exposure to batumin resulted in a statistically significant increase in the number of HaCat cells occupying the sub-G_1 phase to 14% when compared to the vehicle-treated cells

(3%). Mupirocin-treated HaCat samples demonstrated a significant decrease in percentage of cells occupying the G_1 phase to 54% when compared to vehicle-treated cells (61%) and a decrease in the G_2/M phase to 14% when compared to vehicle-treated cells (22%). Mupirocin-treated UCT MEL-1 samples showed a significant decrease in the percentage of cells occupying the G_1 phase to 71% when compared to vehicle-treated cells (80%) and a decrease in percentage of cells occupying the G_2/M phase to 8% compared to vehicle-treated cells (14%). Thus, exposure to mupirocin resulted in slightly more induction of cell death in the skin keratinocytes HaCat cells compared to the melanoma cells. This apparent contradiction with the mupirocin cytotoxicity results (Table 2) will be discussed below. In addition, actinomycin D-treated HaCat cells experienced a significant increase in the sub-G_1 phase to 36% demonstrating a more prominent induction of cell death when compared to exposure to either mupirocin or butamin. However, actinomycin D exposure in the UCT MEL-1 cell line resulted in an increase in the sub-G_1 phase to 14%. Exposure to both antibiotic compounds resulted in a more significant increase in the sub-G_1 phase indicating that these compounds induce cell death to a larger extent.

Melanoma cell morphology

Light microscopy was conducted to assess the effect of the antibiotics on the morphology of UCT-Mel 1 melanoma cells stained by haematoxylin and eosin. Mupirocin and batumin were evaluated at concentrations 4, 8 and 12 µg/ml (Fig. 5) and compared to cells propagated in 1% DMSO in complete DMEM growth medium and cells treated with 0.0008 µg/ml actinomycin D as negative and positive controls. Hypercondensed chromatin, nuclear fragmentation and possible apoptotic body formations were observed when the cells were treated with 4 µg/ml of antibiotics (Fig. 5A-B). Exposure to 8 µg/ml of antibiotics revealed several differences in morphology of the treated cells (Fig. 5C-D). Cell morphology abnormalities resembling autophagosomes (indicated in Fig. 5 by black arrows) and cell blebbing and rounding followed by cell lysis (indicated by white arrows) were observed in both cases. However, the former abnormalities were more characteristic for the cells treated with batumin, while the giant swollen cells were observed predominantly in the mupirocin-treated cells. This difference in cell morphology caused by the treatment with mupirocin and batumin were more prominent when the cells were treated with 12 µg/ml of the antibiotics (Fig. 5E-F). Differences in the morphology of

cells treated with mupirocin and batumin most likely result from different affinity of these antibiotics to target proteins as previously discussed.

Conclusion

This study demonstrated the promising culture-specific cytotoxic activity of mupirocin against UCT-Mel 1 melanoma and, to some extent, against MCF-7 breast cancer cell lines. Mupirocin showed low level of toxicity against HaCat normal skin keratinocytes (IC_{50} = 415.5 μg/ml). These findings suggest a potentiality to use mupirocin or its derivatives for melanoma prophylaxis. Mupirocin was discovered as a selective anti-staphylococcal antibiotic [16-19]. The interest in this antibiotic increased after the emergence and wide distribution of methicillin-resistant staphylococcal infections (MRSA) which remained sensitive to mupirocin [16]. The anti-cancerous effect of mupirocin has never been reported, but it has been discovered recently for another polyene antibiotic batumin [6], which shares the spectrum of activities and molecular targets with mupirocin [10]. The current study has demonstrated that both antibiotics mupirocin and batumin exhibit a similar range of cytotoxic activities against various cancer cell lines with the highest activity against UCT-Mel 1. Nevertheless, observed differences in the cell cycle progression distribution (Fig. 4) and cell death morphology (Fig. 5) imply inhibition of different target proteins by mupirocin and batumin. It resembles the situation with the selective anti-staphylococcal activity of these antibiotics. Computer modelling predicted the ability of these antibiotics to bind to IleRS [10], but only mupirocin showed an inhibition of protein synthesis, while batumin disrupted fatty acid biosynthesis [13].

Cell cycle progression studies showed that mupirocin induced a significant increase in the quantity of cells occupying the sub-G_1 phase in both cell lines indicating the induction of cell death. The impact of mupirocin on the cell cycle progression and the induction of a sub-G_1 peak have not previously been reported in addition to the novel comparison between butamin and mupirocin. Furthermore, no significant cell cycle block was induced at the concentrations and exposure times utilized in this study since there was no significant increase observed in the quantity of cells occupying the G_1, S and G_2/M phases. The G_1 phase refers to the time during which the cell prepares for DNA replication, which occurs during the S phase. G_2 phase refers to the time period where the cell prepares for mitosis which occurs during the M phase.

Various cell cycle checkpoints are in place to ensure the cell cycle occurs only when the cell is in a suitable environment and has adequately completed the previous stages of its cell cycle [39]. Furthermore, data obtained from cell cycle progression differs from data obtained via XTT assay on cytotoxicity since this metabolic assay quantifies the enzyme activities that are associated with cell metabolism and is not a direct indicator of viability or the induction of cell death. The cell cycle progression studies referring to the reduction of cell number via decreased proliferation or induction of cell death greatly contribute and influence data obtained from the metabolic assays [40, 41]. However, it should be noted that exposure to mupirocin did affect the HaCat cells to a greater extent compared to the cancerous cell line UCT Mel-1 (Table 2) in contrast to batumin, which exerted a significantly more prominent effect on the melanoma cells when compared to the HaCat non-tumourigenic skin keratinocytes. Although mechanisms of action utilized by these compounds remain elusive, the induction of cell death by butamin and mupirocin are indicated via cell cycle progression data and future studies will be required to investigate the type of cell death induced as well as the signaling pathways utilized by these compounds and applicability of these compounds on practice. Variety of activities of polyene antibiotics may be explained by the flexibility and plasticity of their molecules. Computer modelling of spatial organizations of molecules revealed 96 stable conformations of mupirocin and 199 conformations of batumin. Only few of these conformations showed high affinity to the target proteins. Polyene antibiotics may interact with proteins by creating hydrogen bonds and by hydrophobic and electrostatic forces. Each conformation is characterized with a unique spatial organization of the chemical groups involving in non-covalent bonding. This structural plasticity creates a vast variety of bioactivities of these compounds, but makes the structure-activity relationship modelling rather difficult [13, 42]. Moreover, a recent study reported a keto-enolic tautomerization of batumin that increases significantly the number of possible conformations of this compound [25]. A significant contribution toward elucidation of bioactivities of kalimantacin/batumin antibiotics through stereochemistry analysis of these molecules was made in a recent publication by Thistlethwaite *et al*. [43].

Fig. 3 illustrates that the effective binding to protein active sites may occur only when the antibiotics are in specific conformations and the optimal conformations of binding to MDM2-p53 were not the same as those produced by binding to Act1. All of them differ from the conformations reported for binding to IleRS [10]. Binding of polyene antibiotics to multiple

molecular targets occurs in a competitive fashion and may depend on the state of the organism (cancerous and normal cells, for example) and also on the concentration of antibiotics. Several recent studies reported that mupirocin has a wider range of bioactivities, which cannot be explained solely by the IleRS inhibition. When applied in sub-lethal concentrations, mupirocin inhibits alpha-toxin production in MRSA by down-regulation of *agr*, *saeRS* and *sarA* genes [44] and it also stimulates biofilm formation in *S. aureus* [45]. Moreover, the natural role of mupirocin in preventing bacteria from amoebal grazing was demonstrated [46]. Mupirocin shows no amoebicidal activity, but it promotes the inhibition of amoeba by the jessenipeptin polypeptide antibiotic produced by the same grazing-resistant bacterium.

The current study showed the ability of mupirocin to interact with cancer-related proteins p53 and Act1. Inhibition of the MDM2-p53 active site can induce an apoptotic response in cancerous cells when an inactivation of Act1 inhibits cell proliferation. Selective cytotoxicity of mupirocin against UCT-Mel 1 melanoma cells was reported in this research and the analysis of the cell morphology and cell cycle progression suggested the involvement of cell death induction and cell growth deregulation. More studies have to be conducted to estimate to which extent the inhibition of p53 and Act1 by mupirocin contributes to the melanoma cell death. It cannot be excluded that other mechanisms and molecular targets may be involved in this process.

Low toxicity of mupirocin against skin cells suggests a possibility to use it for melanoma prophylaxis after sunburns. Mupirocin is used in the topical ointment Bactroban™. Side effects of application of Bactroban including itching, redness, burning and swellings due to allergic reactions were reported as not frequent [17-19]. It demonstrates once again the safety of mupirocin for topical application. At the same time, it should be noted that the efficacy of Bactroban to prevent melanoma has not been studied at all. No recommendations to use Bactroban for cancer prophylaxis were suggested in this paper. We may guess that Bactroban may show little or no efficacy in terms of melanoma prevention, because this ointment was developed specifically for removal of superficial bacterial skin infections [17]. To allow the drug to penetrate skin layers, the formulation of the ointment has to be changed [47]. Moreover, additional studies on the toxicity of the deep inoculation of mupirocin into skin are required. In the current study, cell cycle cytometry studies indicate that mupirocin significantly affect HaCat keratinocytes viability which potentially suggests a possibility for additional side effects after

application of mupirocin in higher dozes than in Bactroban and for longer periods of time required for melanoma treatment of prophylaxis.

Future perspective

Additional studies to assess the potential of the anti-proliferative effect of mupirocin and prospects of its application as a drug for melanoma prophylaxis or treatment should be carried out. Pharmacokinetics of mupirocin and batumin has not been studied in detail as these antibiotics were recommended for the topical application only. The reason for this type of application was that both these compounds bound strongly to blood plasma proteins that reduced their antibacterial activities several orders of magnitude [14]. However, binding of the antibiotics to blood proteins may prevent them from decomposing and prolong their persistence in the organism. Both antibiotics show a significant chemical stability. According the technical documentation of Bactroban™, the shelf life of this ointment at room temperature is 18 months. Lyophilized extracts or water or ethanol solutions of batumin keep activities for several years when shelved at 4°C (not documented personal communication by Dr. Klochko V. V).

In vivo experimentation on laboratory mice transplanted with Lewis lung carcinoma cells demonstrated a significant anti-metastatic activity of batumin [6]. Similar activity of an intravenous administration of mupirocin may be expected and should be evaluated in future studies. A possible synergetic effect of a combinatorial application of mupirocin and batumin may be expected from the fact that the mechanisms of selective cytotoxicity of these antibiotics are not identical that was concluded from the observation of different morphology of cells treated with these antibiotics. An example of synergetic activation of mupirocin and jessenipeptin amoebicidal and antibacterial activities has been reported recently [46]. All these facts make it promising to continue studying these antibiotics in view of creation of innovative medicines for melanoma prophylaxis and treatment using mupirocin and batumin, or their derivatives. With this paper we want to draw attention to this prospective class of bioactive compounds represented here by mupirocin and kalimantacin/batumin, the specter of therapeutic activities of which has not been sufficiently studied yet. Another similar polyketide thiomarinol A is a hybrid molecule of pseudomonic acid and and pyrrothine synthesized by *Pseudoalteromonas* sp. SANK 73390 was reported as antibiotic against MRSA [48]. Anti-cancer activity of this antibiotic has

not been studied. Another candidate to join this class of bacterial secondary metabolites is gephyronic acid synthesized by the myxobacterium *Archangium gephyra*. The chemical structure of this compound is similar to that of mupirocin except for missed central part of mupirocin with the ring structure. Remarkably that gephyronic acid shows strong culture-specific suppression of cancerous cell by inhibition of protein translation [49]. A holistic comparative study of these compounds including the elucidation of affected pathways and targeted regulatory proteins by Western blot and immunohistochemistry; as well as structure-activity modeling may open future broad prospects of development of new drugs for cancer treatment and prophylaxis based on these compounds and their combinations.

Summary Points

- Mupirocin has been used for long time against *S. aureus* in the topical ointment Bactroban^{TM}.

- Mupirocin showed cytotoxicity against UCT-Mel 1 melanoma and MCF-7 human breast cancer cell lines.

- Mupirocin showed low toxicity against HaCat skin keratinocytes that was 77-fold lower than that detected for melanoma cells.

- Performed studies suggested the possibility of apoptosis induction and (PI3K)-Akt signaling pathway inhibition in mupirocin-treated cancer cells.

- Reduced toxicity of mupirocin suggests a potential possibility to use this antibiotic for melanoma prophylaxis and treatment.

Figure legends

Figure 1. The results of docking of chemical structures of mupirocin and batumin against PharmaDB database of protein active centers. The program estimated relative values of affinity in the range from 0 to 1 (axis Y). Results of docking to the structural models of the

MDM2 active center of the protein p53 (2X0U and 2X0V), and the active center of the protein Act1 (2CQW) are shown.

Figure 2. Schematic illustration of molecular bonding of structural components of batumin and mupirocin to amino acids in active centers of possible molecular targets of these antibiotics. Hydrogen atoms were hidden in the chemical structures for simplification. It has to be noted to avoid ambiguities that there are no charged atoms in these structures. Non-covalent bonds were depicted by arrows (hydrogen donor→acceptor), one-side-headed lines (circle at the end indicates the positive site of an electrostatic interaction) and by two-side-headed lines for hydrophobic bonds**.**

Figure 3. Molecular docking of mupirocin and batumin structures to the active sites of proteins MDM2-p53 and Act1. A) Batumin in MDM2-p53; B) Mupirocin in MDM2-p53; C) Batumin in Act1; D) Mupirocin in Act1. Proteins are illustrated as solid ribbons. Molecular structures of ligands and the structures of interacting amino acid residues are depicted by sticks and balls. Conformations of the antibiotics corresponding to the highest binding energy are shown next to the protein docking schemes. Potentiality of ligands' surface areas for hydrogen donor/acceptor bonding is highlighted by color gradient from pink (potential hydrogen donors) to green (potential hydrogen acceptors). Hydrophobic parts of the ligands have grey shading. Ligands' sites participating in interactions with amino acid residues are marked by labeled circles with color shading depicting hydrogen donors (pink), hydrogen acceptors (green), positively charged antibiotics (orange) or by open circles for amino acids participating in hydrophobic interactions.

Figure 4. Histograms depicting cell cycle progression. Skin keratinocyte HaCat cells and melanoma UCT-MEL 1 cells were exposed to 1% DMSO (vehicle), 5.4 µg/ml mupirocin or 4.5 µg/ml batumin and 0.0015 µg/ml actinomycin D as a positive control. The units for the axis X are FL3 Lin fluorescent intensity. Heights of graphs along the axis Y were adjusted automatically by the program. Histograms are a representational cell cycle progression repeat of the 3 experimental repeats.

Figure 5. Haematoxylin and eosin staining of UCT-Mel 1 cells under different treatment regiments. Cells were treated by mupirocin and batumin at 4 µg/ml (A and B); 8 µg/ml (C and

D); 12 µg/ml (E and F); and control cells treated with G) 0.0008 µg/ml actinomycin D and H) 1% DMSO after 72 h of incubation. Cells were observed under 20× and 40× magnification. Cell morphology abnormalities resembling autophagosomes are indicated by black arrows and swollen cells are indicated by white arrows.

Table legends

Table 1. Binding energies predicted by LibDock molecular docking simulation for mupirocin and batumin against the MDM2-p53 and Act1 active centers.

Table 2. Anti-proliferative activity of mupirocin against cancer cell lines A431, UCT-MEL-1, HeLa and MCF-7 and against normal skin keratinocytes HaCat as revealed by XTT in comparison to the anti-proliferative activities of batumin and actinomycin D.

Table 3 Percentage of cells in different cell cycle phases determined by cytometry and Cyflogic 1.2.1 processing.

References

1. Valachovic E, Zurbenko I. Skin cancer, irradiation, and sunspots: the solar cycle effect. *Biomed. Res. Int*. 2014, 538574 (2014).
2. Erdei E, Torres SM. A new understanding in the epidemiology of melanoma. *Expert Rev. Anticancer Ther*. 10, 1811–1823 (2010).
3. Whitaker DK, Sinclair W. Melanoma Advisory Board. Guideline on the management of melanoma. *S. Afr. Med J*. 94, 699-707 (2004).
4. Lucas RM, Norval M, Wright CY. Solar ultraviolet radiation in Africa: a systematic review and critical evaluation of the health risks and use of photoprotection. *Photochem. Photobiol. Sci*. 15, 10-23 (2016).
5. Cuzick J, Powles T, Veronesi U, Forbes J, Edwards R, Ashley S, Boyle P. Overview of the main outcomes in breast-cancer prevention trials. *Lancet*. 361, 296-300 (2003).
6. Soldatkina MA, Klochko VV, Zagorodnya SD, Rademan S, Visagie MH, Lebelo MT, Gwangwa MV, Joubert AM, Lall N, Reva ON. Promising anti-cancer activity of batumin

– a natural polyene antibiotic produced by *Pseudomonas batumici*. *Future Med. Chem.* 10, 2187-2199 (2018).

7. Mattheus W, Gao LJ, Herdewijn P, Landuyt B, Verhaegen J, Masschelein J, Volckaert G, Lavigne R. Isolation and purification of a new kalimantacin/batumin-related polyketide antibiotic and elucidation of its biosynthesis gene cluster. *Chem. Biol.* 17, 149-159 (2010).

*   **This article gives an overview of kalimantacin/batumin-related antibiotics.**

8. Kiprianova EA, Klochko VV, Zelena LB, Churkina LN, Avdeeva LV. *Pseudomonas batumici* sp. nov., the antibiotic-producing bacteria isolated from soil of the Caucasus Black Sea coast. *Mikrobiol. Z.* 73, 3-8 (2011).

9. Mattheus W, Masschelein J, Gao LJ, Herdewijn P, Landuyt B, Volckaert G, Lavigne R. The kalimantacin/batumin biosynthesis operon encodes a self-resistance iso-form of the FabI bacterial target. *Chem. Biol.* 17, 1067-1071 (2010).

*   **This article explains in detail the biosynthesis of kalimantacin/batumin-related antibiotics.**

10. Klochko VV, Zelena LB, Kim JY, Avdeeva LV, Reva ON. Prospects of a new antistaphylococcal drug batumin revealed by molecular docking and analysis of the complete genome sequence of the batumin-producer *Pseudomonas batumici* UCM B-321. *Int. J. Antimicrob. Agents.* 47, 56-61 (2016).

*   **This article gives an additional information on molecular docking of batumin.**

11. Hughes J, Mellows G. Interaction of pseudomonic acid A with *Escherichia coli* B isoleucyl-tRNA synthetase. *Biochem. J.* 191, 209-219 (1980).

12. Gilbart J, Perry CR, Slocombe B. High-level mupirocin resistance in *Staphylococcus aureus*: evidence for two distinct isoleucyl-tRNA synthetases. *Antimicrob. Agents Chemother.* 37, 32-38 (1993).

13. Lee VE, O'Neill AJ. Batumin does not exert its antistaphylococcal effect through inhibition of aminoacyl-tRNA synthetase enzymes. *Int. J. Antimicrob. Agents.* 49, 121-122 (2017).

14. Sutherland R, Boon RJ, Griffin KE, Masters PJ, Slocombe B, White AR. Antibacterial activity of mupirocin (pseudomonic acid), a new antibiotic for topical use. *Antimicrob. Agents Chemother*. 27, 495-498 (1985).

15. Leyden JJ. Studies on the safety of Bactroban ointment: potential for contact allergy, contact irritation, phototoxicity and photo-allergy. Bactroban (Mupirocin). *Excerpta Medica Current Clinical Practice Series*. 16, 68-71 (1985).

16. Ward A, Campoli-Richards DM. Mupirocin. A review of its antibacterial activity, pharmacokinetic properties and therapeutic use. *Drugs*. 32, 425-444 (1986).

17. Jackson D, Tasker TC, Sutherland R, Mellows G, Cooper DL. Clinical pharmacology of Bactroban: pharmacokinetics, tolerance and efficacy studies. In Dobson *et al*. (Eds) Bactroban (mupirocin), pp. 54–66, Excerpta Medica, Amsterdam, 1985.

18. White DG, Collins PO, Rowsell RB. Topical antibiotics in the treatment of superficial skin infections in general practice – a comparison of mupirocin with sodium fusidate. *J. Infection*. 18, 221-229 (1989).

19. Pappa KA. The clinical development of mupirocin. *J. American Acad. Dermatology*. 22, 873-879 (1990).

20. Thomas CM, Hothersall J, Willis CL, Simpson TJ. Resistance to and synthesis of the antibiotic mupirocin. *Nat. Rev. Microbiol*. 8, 281-289 (2010).

21. El-Sayed AK, Hothersall J, Cooper SM, Stephens E, Simpson TJ, Thomas CM. Characterization of the mupirocin biosynthesis gene cluster from *Pseudomonas fluorescens* NCIMB 10586. *Chemistry & Biology*. 10, 419-430 (2003).

22. Hamilton-Miller JM. Chemistry and biology of the polyene macrolide antibiotics. *Bacteriol. Rev*. 37, 166-196 (1973).

** **This article gives an overview of mechanisms of action of various polyene antibiotics.**

23. Gomes ES, Schuch V, de Macedo Lemos EG. Biotechnology of polyketides: new breath of life for the novel antibiotic genetic pathways discovery through metagenomics. *Braz. J. Microbiol*. 44, 1007-1034 (2014).

24. Woerly EM, Roy J, Burke MD. Synthesis of most polyene natural product motifs using just 12 building blocks and one coupling reaction. *Nat. Chem*. 6, 484-491 (2014).

25. Klochko V.V. Biosynthesis and properties of antibiotic batumin. Biotech. Acta 7, 46-50 (2014).

26. Meslamani J, Rognan D. Protein-Ligand Pharmacophores: Concept, Design and Applications. *CICSJ Bulletin*. 33, 27 (2015).

27. Diller DJ, Merz KM Jr. High throughput docking for library design and library prioritization. *Proteins* 43, 113-124 (2001).

28. Berman HM, Westbrook J, Feng Z, Gilliland G, Bhat TN, Weissig H, Shindyalov IN, Bourne PE. The protein data bank. *NAR* 28, 235-242 (2000).

29. Zheng, Y.T., Chan, W.L., Chan, P., Huang, H. and Tam, S.C. Enhancement of the anti-herpetic effect of trichosanthin by acyclovir and interferon. *FEBS Letters* 496, 139-142 (2001).

30. Kirk JM. The mode of action of actinomycin D. *Biochimica et Biophysica Acta* 42, 167- 169 (1960).

31. Lillie RD. Histopathologic technic and practical histochemistry. *McGaw-Hill Book Co.*, New York, 445 (1965).

32. Kroemer G, Galluzzi L, Vandenabeele P, Abrams J, Alnemri ES, Baehrecke EH, Blagosklonny MV, El-Deiry WS, Golstein P, Green DR, Hengartner M, Knight RA, Kumar S, Lipton SA, Malorni W, Nuñez G, Peter ME, Tschopp J, Yuan J, Piacentini M, Zhivotovsky B, Melino G; Nomenclature Committee on Cell Death 2009. Classification of cell death: recommendations of the Nomenclature Committee on Cell Death 2009. *Cell Death Differ*. 16, 3-11 (2009).

33. Riccardi C, Nicoletti I. Analysis of apoptosis by propidium iodide staining and flow cytometry. *Nat. Protoc*. 1, 1458-1461 (2006).

34. Bézivin C, Tomasi S, Lohézic-Le Dévéhat F, Boustie J. Cytotoxic activity of some lichen extracts on murine and human cancer cell lines. *Phytomedicine* 10, 499-503 (2003).

35. Yu M, Wang Y, Zhu J, Bartberger MD, Canon J, Chen A, Chow D, Eksterowicz J, Fox B, Fu J, Gribble M, Huang X, Li Z, Liu JJ, Lo MC, McMinn D, Oliner JD, Osgood T, Rew Y, Saiki AY, Shaffer P, Yan X, Ye Q, Yu D, Zhao X, Zhou J, Olson SH, Medina JC, Sun D. Discovery of potent and simplified piperidinone-based inhibitors of the MDM2-p53 interaction. *ACS Med. Chem. Lett*. 5, 894-899 (2014).

36. Addie M, Ballard P, Buttar D, Crafter C, Currie G, Davies BR, Debreczeni J, Dry H, Dudley P, Greenwood R, Johnson PD, Kettle JG, Lane C, Lamont G, Leach A, Luke RW, Morris J, Ogilvie D, Page K, Pass M, Pearson S, Ruston L. Discovery of 4-amino-N-[(1S)-1-(4-chlorophenyl)-3-hydroxypropyl]-1-(7H-pyrrolo[2,3-d]pyrimidin-4-yl) piperidine-4-carboxamide (AZD5363), an orally bioavailable, potent inhibitor of Akt kinases. *J. Med. Chem.* 56, 2059-2073 (2013).

37. Vaupel A, Bold G, De Pover A, Stachyra-Valat T, Lisztwan JH, Kallen J, Masuya K, Furet P. Tetra-substituted imidazoles as a new class of inhibitors of the p53-MDM2 interaction. *Bioorg. Med. Chem. Lett*. 24, 2110-2114 (2014).

38. Zhang Q, Zeng SX, Lu H. Targeting p53-MDM2-MDMX loop for cancer therapy. *Subcell. Biochem*. 85, 281-319 (2014).

39. Seaton DD, Krishan J. Model-based analysis of cell cycle responses to dynamically changing environments. *Plos Comput. Biol*. 12, e1004604 (2016).

**   This article gives an overview of eukaryotic cell cycle responses to different conditions and stimuli.

40. Berridge MV, Herst P, Tan AS. Tetrazolium dyes as tools in cell biology: new insights into their cellular reduction. Biotechnol. Annu. Rev. 11, 127-152 (2005).

41. Śliwka, L, Wiktorska K, Suchocki P, Milczarek M, Mielczarek S, Lubelska, K, Cierpiał T, Łyżwa P, Kiełbasiński P, Jaromin A, Flis A, Chilmonczyk Z. The comparison of MTT and CVS assays for the assessment of anticancer agent interactions. *Plos One* 11, e0155772 (2016).

**   This article verifies different anticancer activity assays and identifies sources of discrepancies.

42. Valeriote F, Medoff G, Dieckman J. Potentiation of cytotoxicity of anticancer agents by several different polyene antibiotics. *J. Natl. Cancer Inst*. 72, 435-439 (1984).

43. Thistlethwaite IRG, Bull FM, Cui C, Walker PD, Gao SS, Wang L, Song Z, Masschelein J, Lavigne R, Crump MP, Race PR, Simpson TJ, Willis CL. Elucidation of the relative and absolute stereochemistry of the kalimantacin/batumin antibiotics. *Chem. Sci*. 8, 6196-6201 (2017).

***	This article elucidates properties and activities of kalimantacin/batumin-related antibiotics through their stereochemistry.**

44.	Jin Y, Li M, Shang Y, Liu L, Shen X, Lv Z, Hao Z, Duan J, Wu Y, Chen C, Pan J, Yu F. Sub-inhibitory concentrations of mupirocin strongly inhibit alpha-toxin production in high-level mupirocin-resistant MRSA by down-regulating *agr*, *saeRS*, and *sarA*. *Front. Microbiol*. 9, 993 (2018).

45.	Sritharadol R, Hamada M, Kimura S, Ishii Y, Srichana T, Tateda K. Mupirocin at subinhibitory concentrations induces biofilm formation in *Staphylococcus aureus*. *Microb. Drug Resist*. doi: 10.1089/mdr.2017.0290. [Epub ahead of print] (2018).

46.	Arp J, Götze S, Mukherji R, Mattern DJ, García-Altares M, Klapper M, Brock DA, Brakhage AA, Strassmann JE, Queller DC, Bardl B, Willing K, Peschel G, Stallforth P. Synergistic activity of cosecreted natural products from amoebae-associated bacteria. *Proc Natl Acad Sci U S A*. 115, 3758-3763 (2018).

47.	Trommer H, Neubert RH. Overcoming the stratum corneum: the modulation of skin penetration. A review. *Skin Pharmacol. Physiol*. 19, 106-121 (2006).

48.	Fukuda D, Haines AS, Song Z, Murphy AC, Hothersall J, Stephens ER, Gurney R, Cox RJ, Crosby J, Willis CL, Simpson TJ, Thomas CM. A natural plasmid uniquely encodes two biosynthetic pathways creating a potent anti-MRSA antibiotic. *PLoS One*. 6, e18031 (2011).

49.	Muthukumar Y, Münkemer J, Mathieu D, Richter C, Schwalbe H, Steinmetz H, Kessler W, Reichelt J, Beutling U, Frank R, Büssow K, van den Heuvel J, Brönstrup M, Taylor RE, Laschat S, Sasse F. Investigations on the mode of action of gephyronic acid, an inhibitor of eukaryotic protein translation from myxobacteria. PLoS One 13, e0201605 (2018).
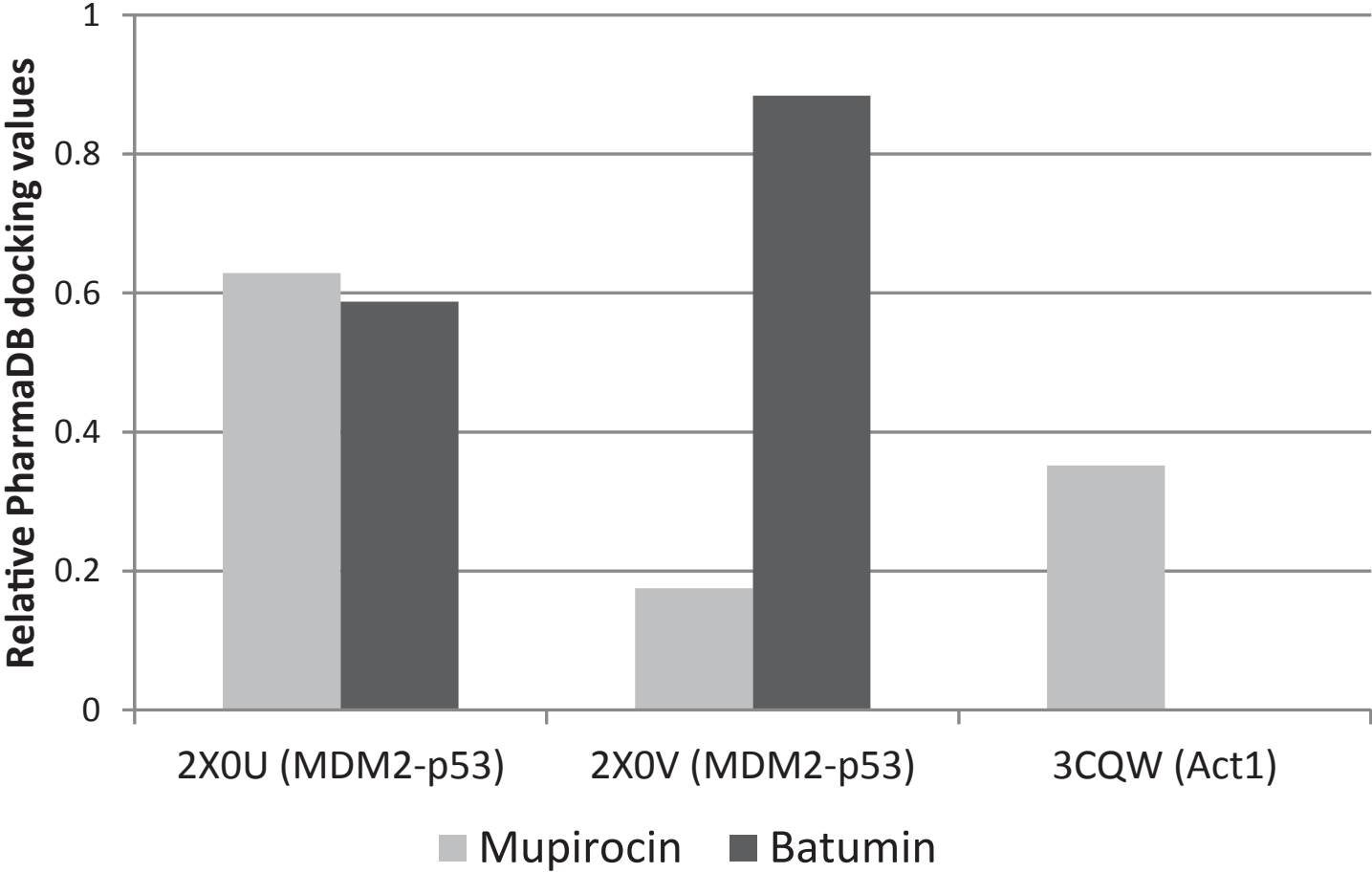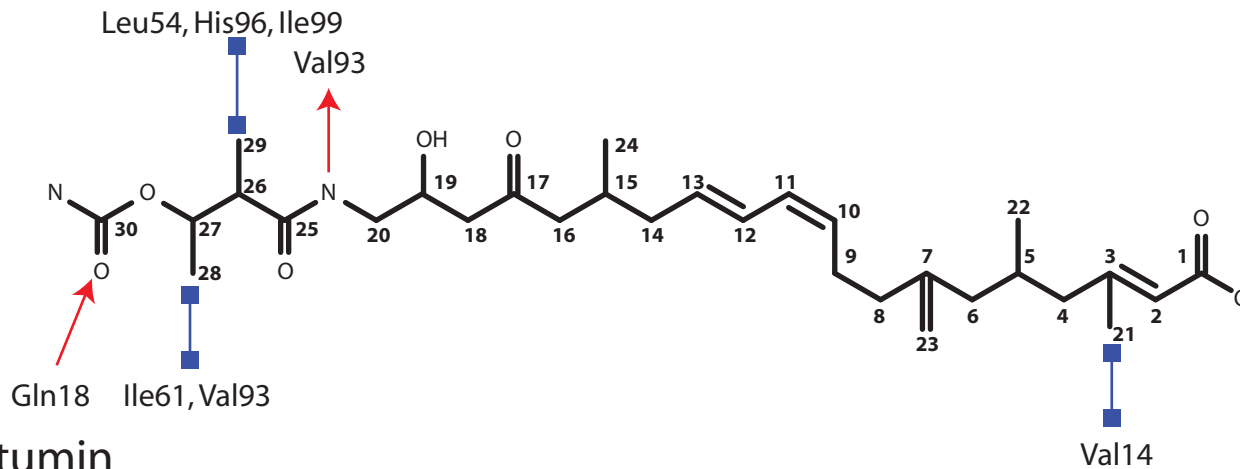
Batumin
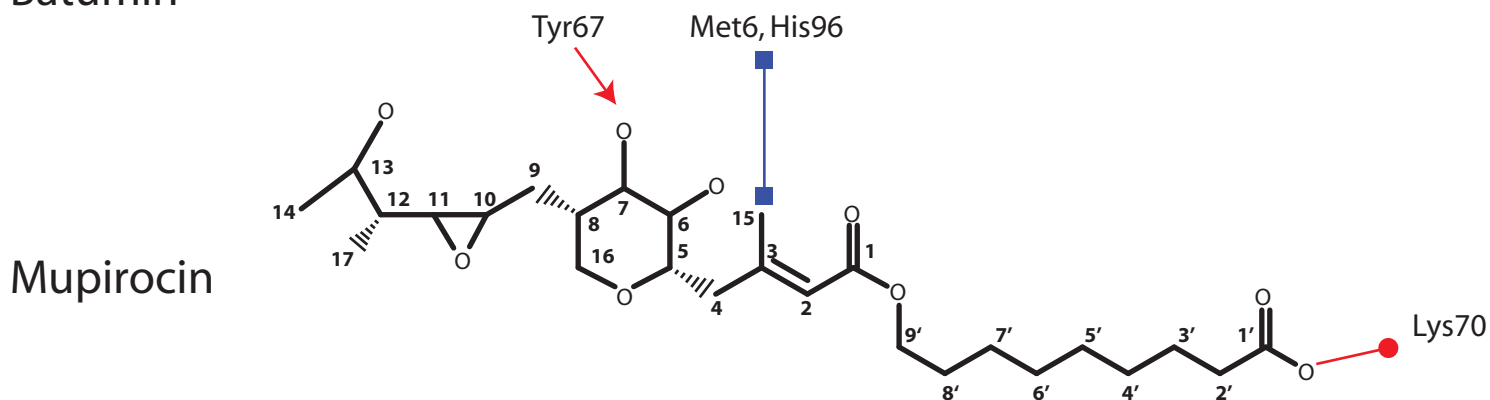
Mupirocin

A) 4QO4 (MDM2-p53)
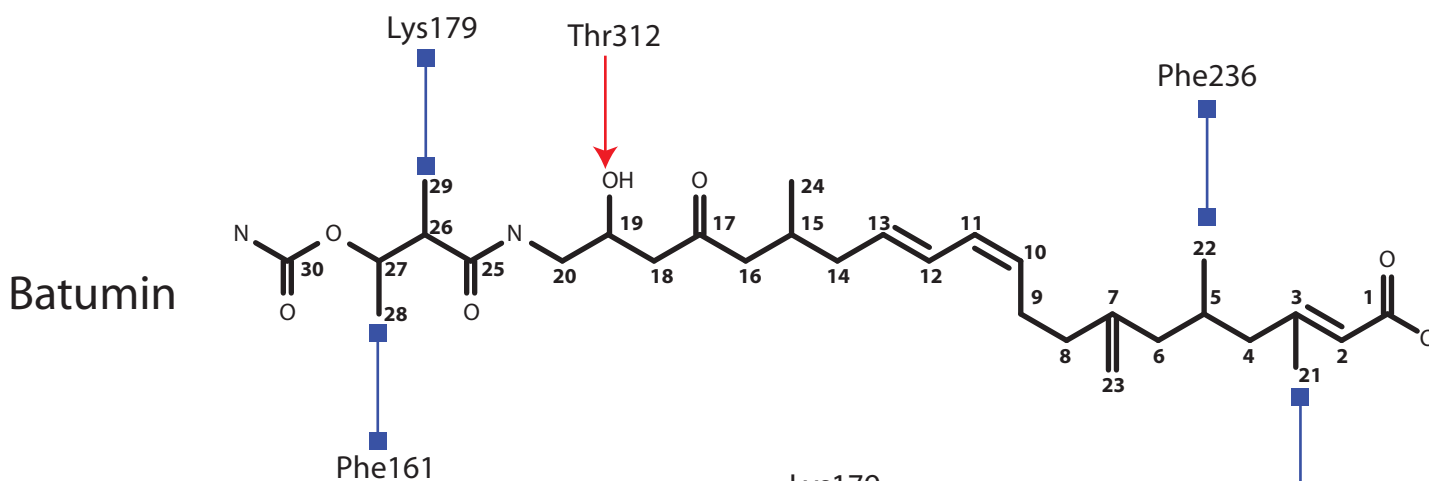
Batumin
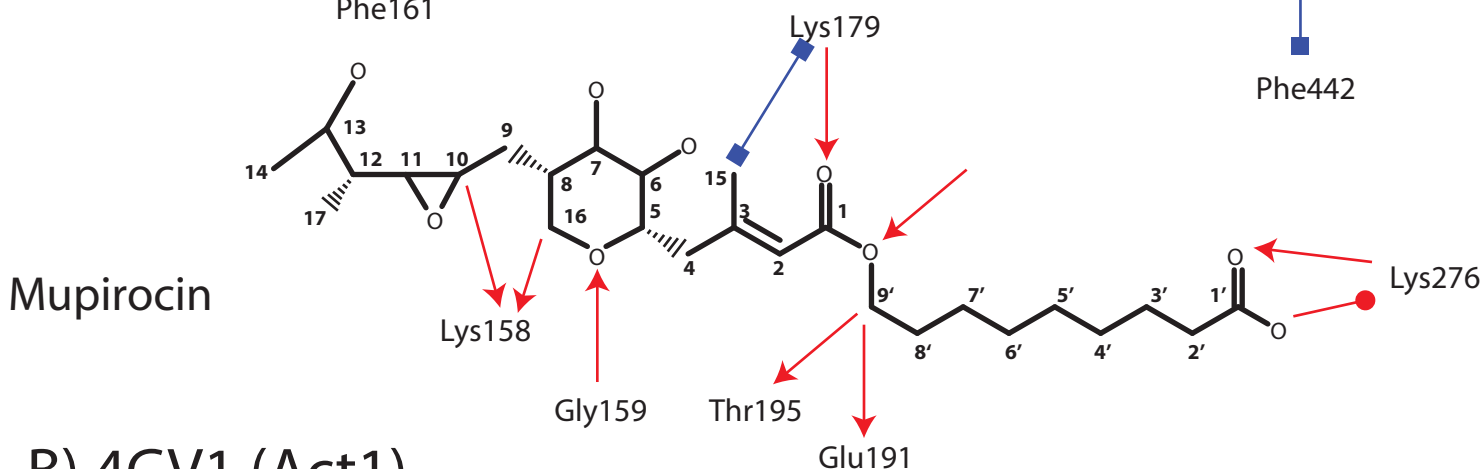
Mupirocin

B) 4GV1 (Act1)
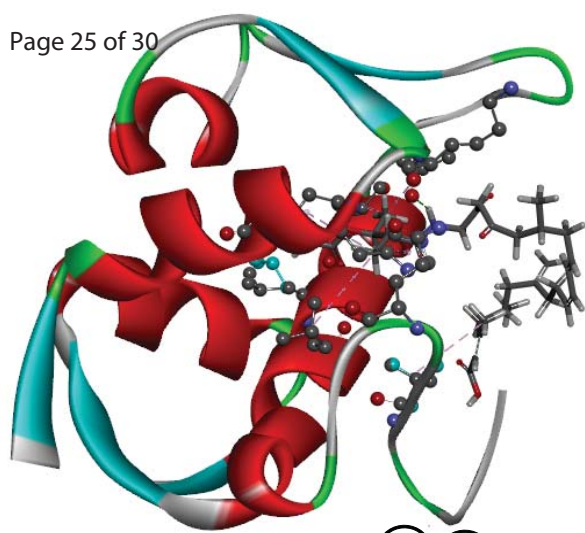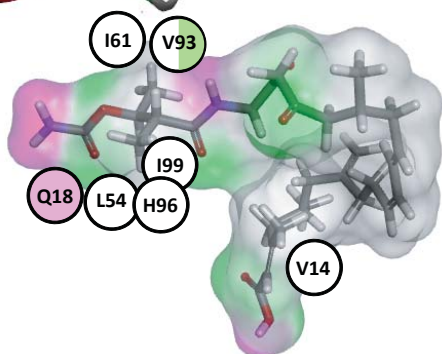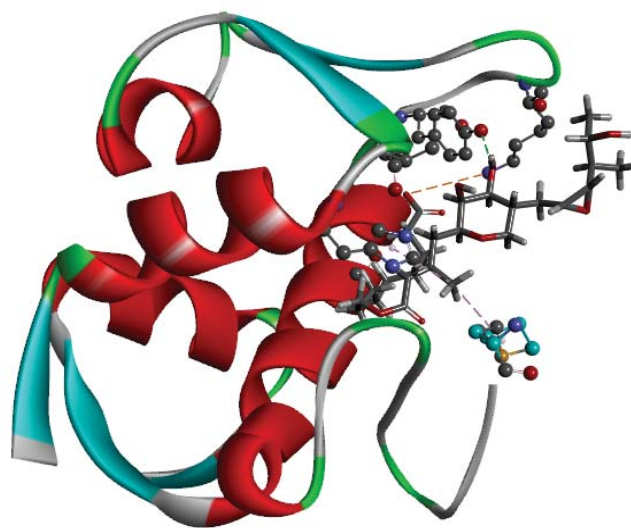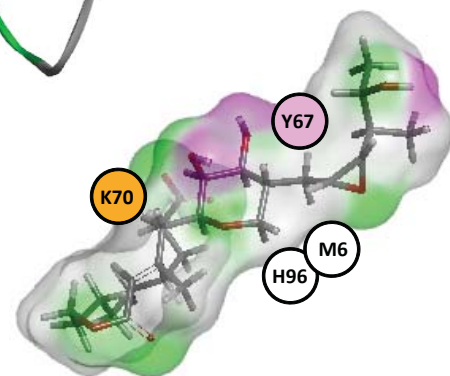
A) Batumin in MDM2-p53;

B) Mupirocin in MDM2-p53;
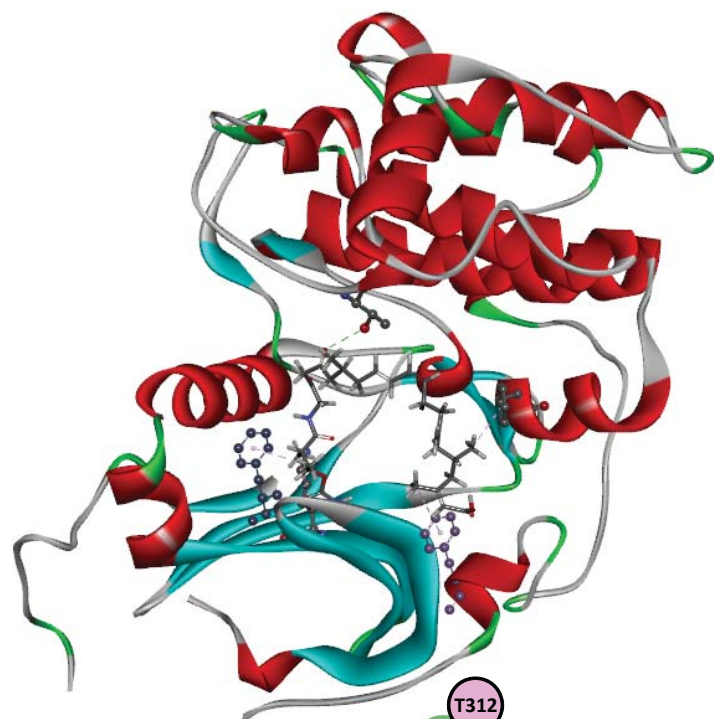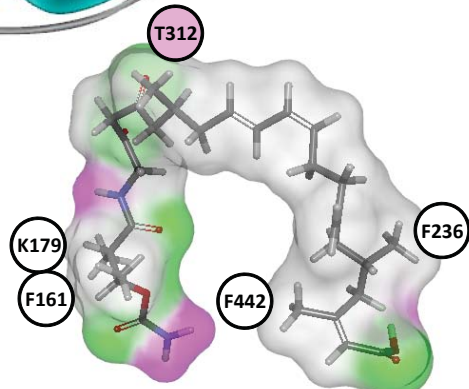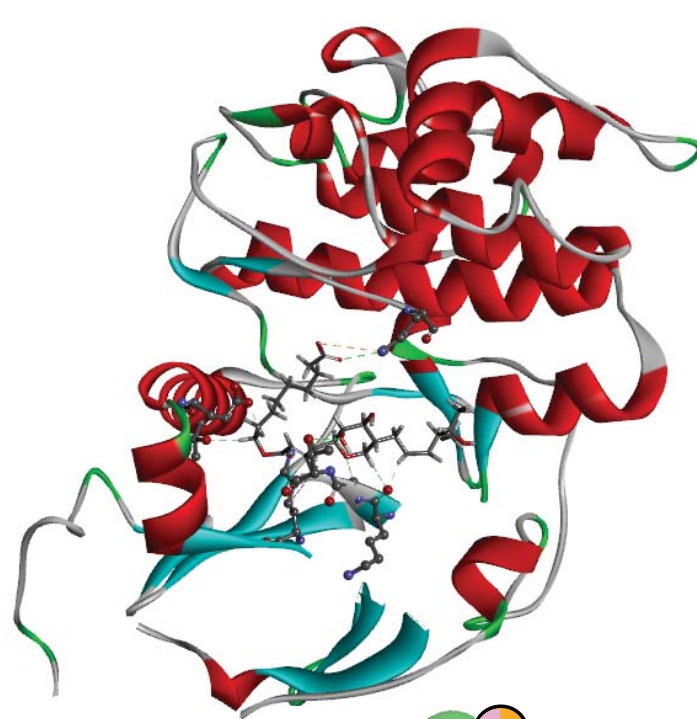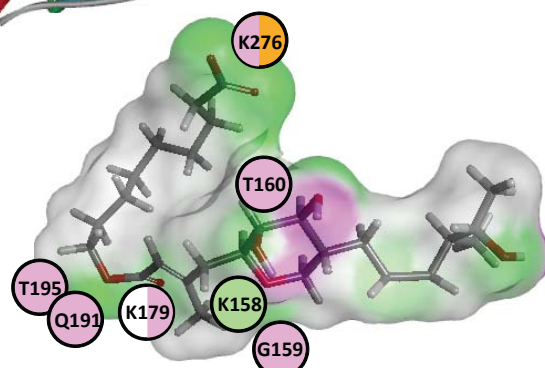
**C) Batumin in Act1;**

D) Mupirocin in Act1;
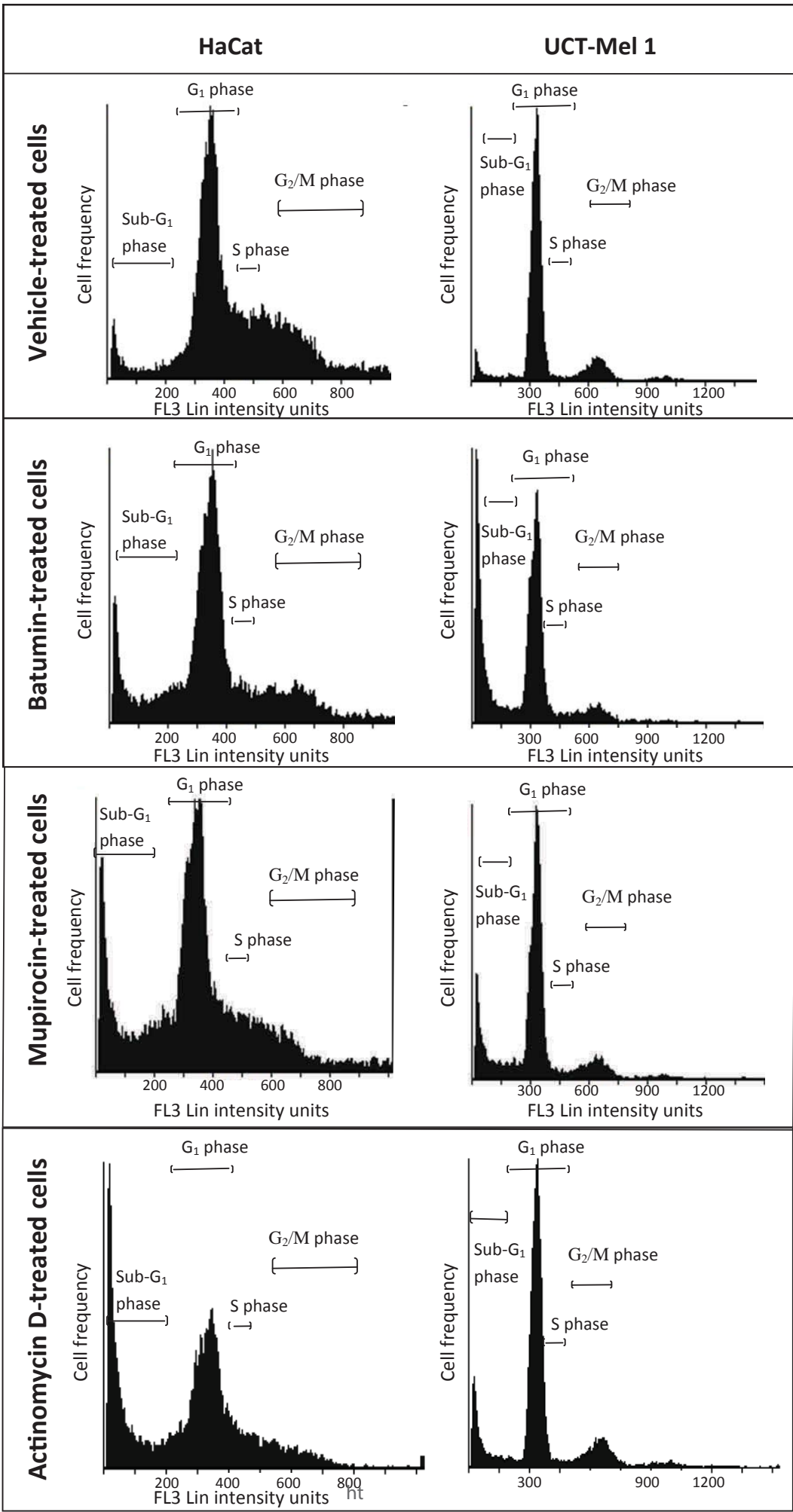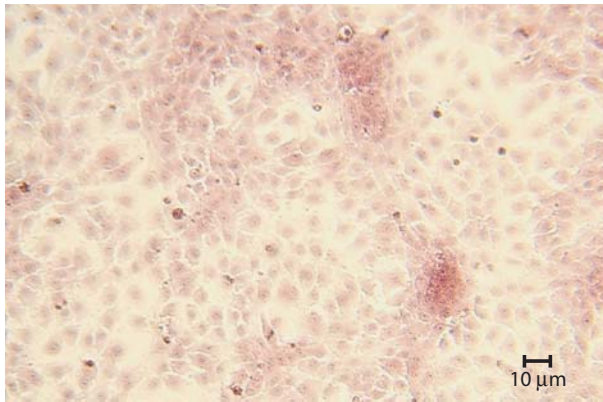
A) Mupirocin 4 µg/ml
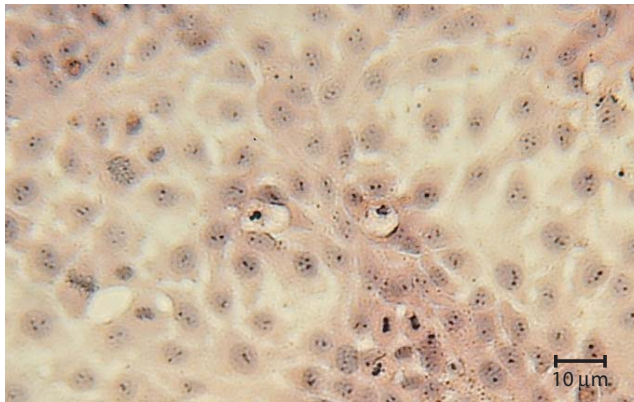
B) Batumin 4 µg/ml
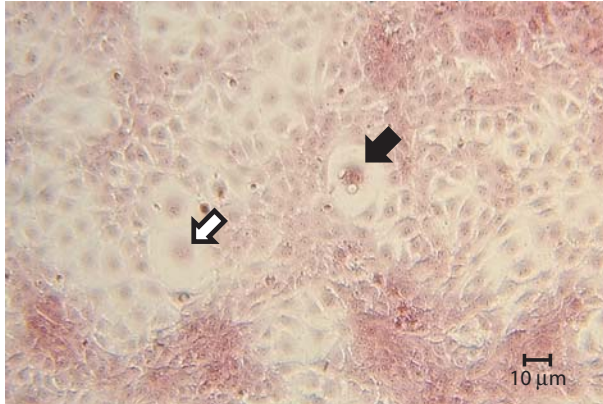
C) Mupirocin 8 µg/ml
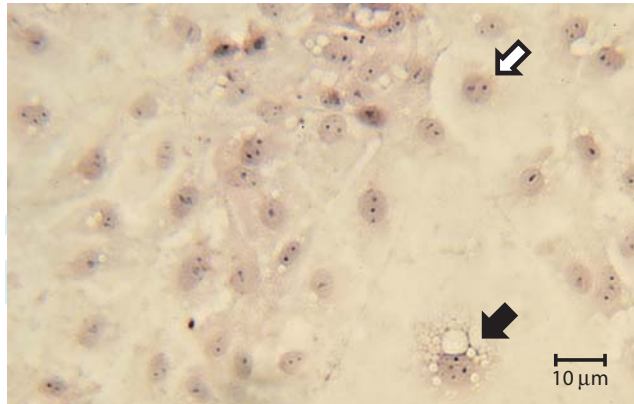
D) Batumin 8 µg/ml
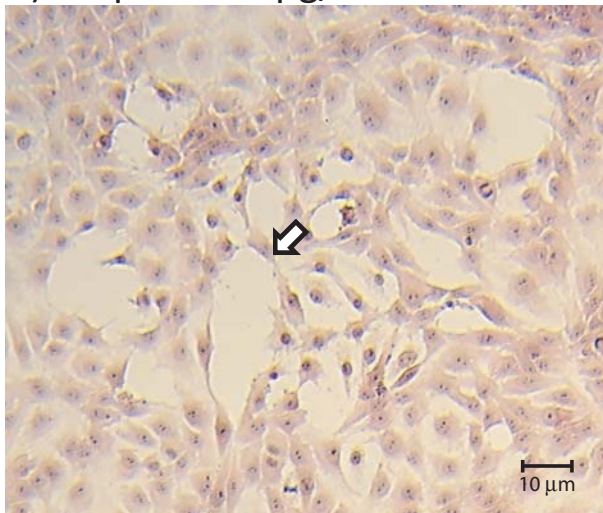
E) Mupirocin 12 µg/ml
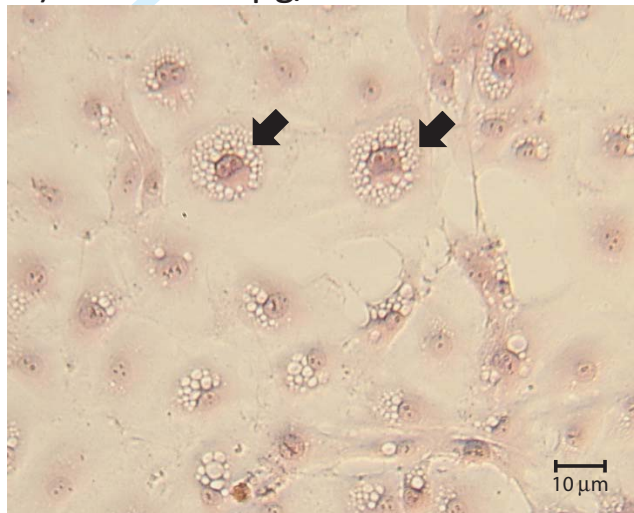
F) Batumin 12 µg/ml
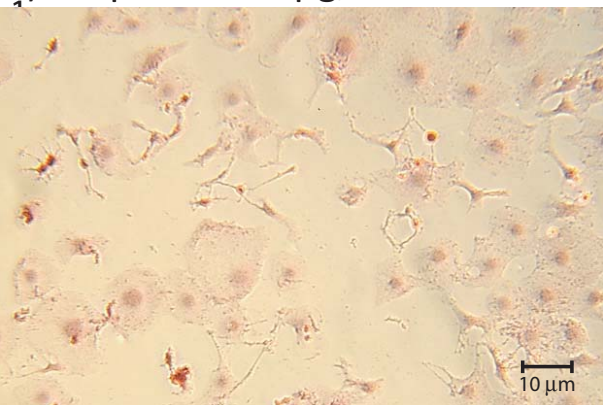
G) Actinomycin 0.0008 µg/ml
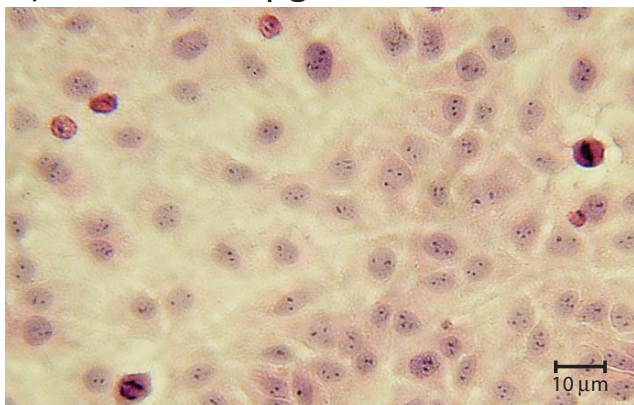
H) 1% DMSO control

Table 1. Binding energies predicted by LibDock molecular docking simulation for mupirocin and batumin against the MDM2-p53 and Act1 active centers.

	Binding energy to molecular targets (kJ/mol)	
	p53	Act1
Mupirocin	47.7	55
Batumin	50	33.6

Table 2. Anti-proliferative activity of mupirocin against cancer cell lines A431, UCT-MEL-1, HeLa and MCF-7 and against normal skin keratinocytes HaCat as revealed by XTT in comparison to the anti-proliferative activities of batumin and actinomycin D.

Cell line	Mupirocin IC$_{50}$ (μg/ml) $\pm$ SD	Batumin IC$_{50}$ (μg/ml) $\pm$ SD	Actinomycin D IC$_{50}$ (μg/ml) $\pm$ SD
A431 – Squamous cell carcinoma	55.9 $\pm$ 7.9	171.3 $\pm$ 6.8	0.0074 $\pm$ 3.6
UCT-Mel 1 – Melanoma skin cancer	5.4 $\pm$ 3.3	4.5 $\pm$ 2.7	0.0073 $\pm$ 3.7
MCF-7 – Breast cancer	35.5 $\pm$ 7.9	140.6 $\pm$ 6.9	0.0082 $\pm$ 5.6
HeLa – Cervical cancer	61.65 $\pm$ 10.0	128.5 $\pm$ 3.7	0.0093 $\pm$ 6.1
HaCat – Skin keratinocytes	415.5 $\pm$ 7.0	101.4 $\pm$ 16.7	0.0018 $\pm$ 7.6

Table 3 Percentage of cells in different cell cycle phases determined by cytometry and Cyflogic 1.2.1 processing.

Cell lines	Sub-G_1 phase	G_1 phase	S phase	G_2/M phase
HaCat				
Vehicle-treated cells	2.93±1.66	61.01±2.07	13.68±1.63	22.37±1.22
Mupirocin-treated cells	20.85±1.17*	54.22±3.51*	11±1.74	13.93±2.53*
Batumin-treated cells	14.14±1.32*	58.80±1.55	8.87±1.54*	18.2±1.31*
Actinomycin D-treated cells	36.36±2.13*	44.25±3.56*	9.68±4.12	9.62±2.13*
UCT-MEL 1				
Vehicle-treated cells	2.73±0.65	80.07±1.8	3.05±0.75	14.14±2.13
Mupirocin-treated cells	16.25±0.83*	71.39±1.57*	4.03±0.49	8.33±1.02*
Batumin-treated cells	38.66±2.21*	51.22±0.99*	2.59±0.7	7.53±1.94*
Actinomycin D-treated cells	13.95±1.2*	74.8±5.12	2.07±1.25	9.16±4.56

*Statistically reliable difference ($P \leq 0.05$) in numbers of cells present in the given cell cycle phase in the batumin-treated cells compared to the vehicle-treated cells.